Ablation of the scaffold protein JLP causes reduced fertility in male mice

doi: 10.1007/s11248-008-9191-6

Full-length Research paper

Ablation of the scaffold protein JLP causes reduced fertility in male mice

Asuka Iwanaga[1]#, Guangmin Wang[1]#, Davaakhuu Gantulga[1], Tokiharu Sato[1], Tuvshintugs Baljinnyam[1], Keiko Shimizu[2], Ken Takumi[2], Motoharu Hayashi[2], Takuya Akashi[3], Hideki Fuse[3], Kazushi Sugihara[4], Masahide Asano[4], Katsuji Yoshioka[1]*

[1]Division of Molecular Cell Signaling, Cancer Research Institute, Kanazawa University, Kanazawa 920-0934, Japan

[2]Department of Cellular and Molecular Biology, Primate Research Institute, Kyoto University, Inuyama 484-8506, Japan

[3]Department of Urology, Graduate School of Medicine and Pharmaceutical Sciences for Research, University of Toyama, Toyama 930-0194, Japan

[4]Division of Transgenic Animal Science, Advanced Science Research Center, Kanazawa University, Kanazawa 920-8640, Japan

#These authors contributed equally to this study.

*Corresponding author: Division of Molecular Cell Signaling, Department of Molecular and Cellular Biology, Cancer Research Institute, Kanazawa University, 13-1 Takara-machi, Kanazawa, Ishikawa 920-0934, Japan

Tel/Fax: +81-76-234-4532

E-mail address: katsuji@kenroku.kanazawa-u.ac.jp

Abstract

The specific and efficient activation of mitogen-activated protein kinase (MAPK) signaling modules is mediated, at least in part, by scaffold proteins. c-Jun NH_2-terminal kinase (JNK)-associated leucine zipper protein (JLP) was identified as a scaffold protein for JNK and p38 MAPK signaling modules. JLP is expressed nearly ubiquitously and is involved in intracellular signaling pathways, such as the $G_{\alpha 13}$ and Cdo-mediated pathway, in vitro. To date, however, JLP expression has not been analyzed in detail, nor are its physiological functions well understood. Here we investigated the expression of JLP in the mouse testis during development. Of the tissues examined, JLP was strongest in the testis, with the most intense staining in the elongated spermatids. Since the anti-JLP antibody used in this study can recognize both JLP and sperm-associated antigen 9 (SPAG9), a splice variant of JLP that has been studied extensively in primates, we also examined its expression in macaque testis samples. Our results indicated that in mouse and primate testis, the isoform expressed at the highest level was JLP, not SPAG9. We also investigated the function of JLP by disrupting the *Jlp* gene in mice, and found that the male homozygotes were subfertile. Taken together, these observations may suggest that JLP plays an important role in testis during development, especially in the production of functionally normal spermatozoa.

Keywords JLP; MAP kinase; knockout mouse; scaffold protein; signal transduction; SPAG9

Introduction

Scaffold proteins of mammalian MAP kinase (MAPK) cascades are thought to be involved in the spatio-temporal regulation of these pathways by organizing the MAPK signaling components into functional modules (reviewed in Morrison and Davis, 2003; Yoshioka, 2004; Dhanasekaran, et al. 2007). The scaffolding complexes enable the efficient activation of specific MAPK modules as well as the protection of the components within the relevant MAPK modules from irrelevant stimuli. Nearly 20 proteins so far have been proposed as scaffolding proteins for mammalian MAPK signaling pathways.

c-Jun NH_2-terminal kinase (JNK)-associated leucine zipper protein (JLP) was originally identified as a binding protein for the transcription factor Max, and was suggested to function as a scaffold protein for the JNK and p38 MAPK signaling modules (Lee et al., 2002). JLP, which is expressed fairly ubiquitously, shares significant sequence identity with JNK/stress-activated protein kinase-associated protein 1 [JSAP1, or JNK-interacting protein 3 (JIP3)], a scaffold protein for JNK cascades (Ito et al., 1999; Ito et al., 2000; Kelkar et al., 2000). Nguyen et al. (2005) showed that JLP physically interacts with kinesin light chain 1, and Kashef et al. (2005) showed that it interacts with $G_{\alpha 13}$, the α-subunit of the heteromeric G_{13} protein. These studies suggested that JLP is involved in the kinesin-mediated spatial regulation of MAPK modules and $G_{\alpha 13}$ signaling pathways, as a scaffold protein. In addition, in vitro evidence suggests that JLP also plays an important role during myogenesis by interacting with the cell-surface protein Cdo (Takaesu et al., 2006). To date, however, the in vivo physiological functions of JLP remain largely unknown.

Some reports on the expression patterns of a splice variant of JLP, SPAG9 (sperm-associated antigen 9) in primates, including human and macaque, showed that SPAG9 is expressed exclusively in the testis, where it is localized to the acrosome of spermatozoa (Shankar et al., 1998; Shankar et al., 2004; Jagadish et al., 2005a and 2005b). All the studies on SPAG9 so far have been done in primates. Recently, Kelkar et al. (2005)

identified a third splice-variant of the *J1p* gene (Kelkar et al., 2005), JIP4. This JIP3-related protein is expressed ubiquitously or nearly so, like JLP.

In the present study, we examined the expression of JLP and SPAG9 in the testes of mouse and macaque, and investigated the physiological function of JLP in mouse by generating and analyzing a *Jlp*-deficient line.

Materials and methods

Animals

All the experiments involving animals were conducted according to the Fundamental Guidelines for Proper Conduct of Animal Experiments and Related Activities in Academic Research Institutions under the jurisdiction of the Ministry of Education, Culture, Sports, Science and Technology of Japan, the Guide for the Care and Use of Laboratory Animals established by the US National Institutes of Health (1985), and the Guide for the Care and Use of Laboratory Primates (2002) established by the Primate Research Institute of Kyoto University. Mice were kept in an environmentally controlled clean room at the Institute for Experimental Animals, Advanced Science Research Center, Kanazawa University. C57BL/6J mice were purchased from SLC (Hamamatsu, Japan). Two reproductive-age male monkeys, a 70-month-old Japanese macaque and a 96-month-old Rhesus macaque, were used for immunohistochemical and Western blotting analyses, respectively. The monkeys were bred and kept in good health at the Primate Research Institute of Kyoto University.

Targeted disruption of the mouse *Jlp* gene

An 8.7-kb genomic region, from 4.5-kb upstream of exon 1 to 4.2-kb downstream of exon 1 of the mouse *Jlp* gene, was used to construct the targeting vector (Fig. 1a). A 3.1-kb (from 4.5-kb to 1.4-kb upstream of exon 1) and a 3.4-kb (0.8-kb to 4.2-kb downstream of exon 1) genomic fragment were amplified by polymerase chain reaction (PCR), and used for left and right arms of the targeting vector, respectively. A neomycin-resistance cassette (neo), the PGK promoter-driven neomycin-resistance gene (Fiedrich and Soriano, 1991), was inserted between the left and right arms, from which exon 1 of the mouse *Jlp* gene had been

completely deleted. The *diphtheria* toxin-A (DT-A) gene (Yagi et al., 1993) was introduced for negative selection. The targeting vector was linearized with *Not*I, and gene targeting using 129/Ola E14-1 ES cells was performed as described previously (Asano et al., 1997; Iwanaga et al., 2007). Homologous recombinants were identified by PCR, and by Southern blotting with the 5'-flanking probe and the neo probe, as shown in Fig. 1a. One ES clone, which contained the targeted mutation allele $Jlp^{tm1Ysok}$, gave rise to a germ-line chimera by the aggregation method (Asano et al., 1997). The mutant mouse was backcrossed to C57BL/6J for three generations, and the resulting mice were used in this study. For PCR-based genotyping, three primers were used: 5'-TGTCAGTTCCGCTGGCTTCGGTA-3' (primer 1), 5'-CTCAGCCTGCAGGCTAAAATCCTG-3' (primer 2), and 5'-TAAAGCGCATGCTCCAGACTGCCTT-3' (primer 3) (nucleotides 79711-79733 and 80231-80254 in GenBank accession no. AL662838 for primers 1 and 2, respectively, and nucleotides 459-474 in GenBank accession no. M18735 for primer 3). Homozygous ($Jlp^{-/-}$) mice were obtained by intercrossing the heterozygous ($Jlp^{+/-}$) mice.

Preparation of cDNAs and quantitative analysis of mRNA

Total RNA was prepared from mouse testis using the RNeasy Protect Mini Kit (Qiagen) according to the manufacturer's instructions, and the RNA samples were treated with RNase-free DNaseI (Promega) to eliminate genomic DNA contamination. cDNAs were synthesized with random hexamers as primers using the Transcriptor First Strand cDNA Synthesis Kit (Roche). Real-time reverse-transcription PCR (RT-PCR) was carried out as described previously (Sato et al., 2005). The expression level of each mRNA was normalized with respect to that of *Gapdh* mRNA. The following three primers, Primer 1, Primer 2, and Primer 3 (see Figure 5a), were used for RT-PCR analysis of the *Jlp* and *Spag9* mRNAs: 5'-GAGCATGTGTTTACAGATCCACTG-3' (Primer 1),

5’-CATTTTCTGAGCTTCTTCTCTCGC-3’ (Primer 2), and 5’-CATTTTCTGAGCTTCTTCTCTCGC-3’ (Primer 3) (nucleotides 2866-2889 and 2992-3015 in GenBank accession no. AF327451 for Primers 1 and 2, respectively, and nucleotides 587-610 in GenBank accession no. AB367798 for Primers 3).

Expression plasmids

The entire coding region for mouse JLP (GenBank accession no. AF327451) was amplified by PCR. The product, which contains an *Eco*RI site at the 5’ end and a stop codon followed by an *Xho*I site at the 3’ end of the sense strand, was digested with *Eco*RI and *Xho*I, and subcloned into *Eco*RI/*Xho*I-digested pcDNA3-Flag (Ito et al., 1999) to generate pcDNA3-Flag-JLP. A portion of the mouse SPAG9 cDNA, encoding the carboxy-terminal region, was amplified by nested PCR, because the amount of SPAG9 mRNA was very low. The nucleotide sequence was deposited in DDBJ/EMBL/GenBank under accession no. AB367798. The entire coding sequence of mouse SPAG9 cDNA (GenBank accession nos. AF327451 and AB367798) was obtained by overlapping PCR. The product, containing an *Eco*RI site at the 5’ end of the sense strand and a stop codon followed by an *Xho*I site at the 3’ end, was digested with *Eco*RI and *Xho*I, and subcloned into *Eco*RI/*Xho*I-digested pcDNA3-Flag to generate pcDNA3-Flag-SPAG9. Both plasmids, pcDNA3-Flag-JLP and pcDNA3-Flag-SPAG9, were used as mammalian expression vectors for Flag-tagged JLP and SPAG9, respectively. The mammalian expression plasmid for Flag-JSAP1 was described previously (Ito et al., 1999).

To generate expression plasmids for JLP glutathione S-transferase (GST) and His fusion proteins, the region encoding amino acid residues 796-955 of JLP was amplified by PCR with two different primer sets. The products, which contained *Eco*RI or *Nhe*I sites at the 5’ ends of the sense strands and stop codons followed by *Xho*I sites at their 3’ ends, were double-digested with *Eco*RI and *Xho*I or *Nhe*I and *Xho*I, and subcloned into

*Eco*RI/*Xho*I-digested pGEX4T-3 (GE Healthcare) and *Nhe*I/*Xho*I-digested pREST-B (Invitrogen) to generate pGEX4T-3-JLP(796-955) and pREST-JLP(796-955), respectively.

Nucleotide sequences of the expression plasmids were confirmed by DNA sequencing.

Antibodies

The GST-JLP (residues 796-955) and His-JLP (residues 796-955) proteins expressed in *Escherichia coli* were purified with glutathione Sepharose (GE Healthcare) and Ni-NTA Agarose (Qiagen) according to the manufacturers' instructions, respectively. The purified GST-JLP protein was injected into Kbl:JW rabbits, and the serum was collected for testing. The antiserum was first absorbed on an immobilized GST-Sepharose column, and the flow-though fraction was further purified with the aid of an antigen-affinity column, the His-JLP-Ni-NTA Agarose column. A portion of the antibody cross-reacting with JSAP1, a family member of JLP, was absorbed on a column immobilized with Flag-JSAP1, which was obtained by transient expression in Human embryo kidney 293T (HEK293T) cells, and the flow-through fraction was used as the anti-JLP antibody in this study. The anti-Flag M2 monoclonal antibody and the anti-actin polyclonal antibody were purchased from Sigma. The antibody to actin (cat. no. A5060) shows a broad specificity with actin isoforms and across a range of organisms. Goat Alexa fluor 488-conjugated anti-rabbit IgG antibody was obtained from Invitrogen. The rabbit polyclonal antibody against phosphorylated and activated JNK (P-JNK) was obtained from Cell Signaling Technology.

Cell culture

HEK293T cells were cultured in Dulbecco's modified Eagle's medium (DMEM, Sigma) supplemented with 10% fetal bovine serum in a 5% CO_2 atmosphere at 37˚C. HEK293T cells (1 X 10^5) in a 35-mm dish were transfected with the expression plasmids for

Flag-tagged proteins using LipoTrust SR (Hokkaido System Science, Japan) according to the manufacturer's instructions. Forty-eight hours after the transfection, the cells were harvested and used for Western blotting analysis. The expression of Flag-tagged proteins in the cultured cells was confirmed by Western blotting using the anti-Flag M2 antibody as described below. Mouse embryonic fibroblasts (MEFs) prepared from *Jlp*$^{+/+}$ and *Jlp*$^{-/-}$ mice were seeded at 5 X 10^5 in a 35-mm dish and cultured using the same conditions as for HEK293T cells. Cells were stimulated with UV-C irradiation, sorbitol (0.3 M, 30 min), or anisomycin (30 μm, 30 min). In the UV-C irradiation experiment, cells in a 35-mm dish were washed once with phosphate-buffered saline (PBS), the PBS was removed, and the cells were exposed to UV-C light at 40 J/m^2 in a CL-1000 Ultraviolet Crosslinker (UVP). The cells were then incubated in medium for 30 min.

Western blotting

Tissues and HEK293T cells were lysed in the following buffer: 50 mM Tris-HCl pH 7.4, 150 mM NaCl, 1 mM EDTA, 0.5% sodium deoxycholate, 0.1% sodium dodecyl sulfate (SDS), and Protease Inhibitor Cocktail (Sigma). For the analysis of P-JNK, the HEK293T cells were lysed in buffer containing 25 mM β-glycerophosphate, 1 mM Na_3VO_4, and 1 mM NaF. Western blotting analysis was carried out as described previously (Sato et al., 2004). The antibodies to JLP, Flag M2, P-JNK, and actin were used at 0.3 μg/ml, a 1:10,000 dilution, a 1:1,000 dilution, and a 1:10,000 dilution, respectively. Protein bands were visualized using Immobilon Western Chemiluminescent HRP Substrate (Millipore). The experiments in Figs. 1c, 2, 4a, 6b, and 7 were performed independently at least three times, and representative results are shown.

Immunohistochemistry

Mice were deeply anesthetized and perfused transcardially with 4% paraformaldehyde (PFA) in phosphate-buffered saline pH 7.4. The testis and epididymis were removed and postfixed overnight at 4˚C, cryoprotected in 30% sucrose, and embedded in OTC compound. The male Japanese macaque was pretreated with ketamine hydrochloride (10 mg/kg, intramuscularly) and deeply anesthetized with pentobarbital sodium (Nembutal, 25 mg/kg, intravenously). Heparin sodium (2 ml, 1000 U/ml) was injected directly into the left ventricle. The animal was first perfused through the ascending aorta with the prewash solution (0.15 M NaCl), and was then perfused with 4% PFA in 0.1 M sodium phosphate buffer pH 7.4. The testis and epididymis were removed and postfixed overnight at 4˚C, cryoprotected in 30% sucrose, and embedded in OTC compound. Sections (10-20-μm thick) were subjected to conventional immunofluorescence by incubation for 1 h at room temperature with 5% bovine serum albumin (Sigma) for blocking, followed by overnight incubation at 4˚C with the primary anti-JLP antibody (1 μg/ml) and a 3-h incubation at room temperature (RT) with the Alexa 488-labeled secondary antibody (1:1000). TOTO-3 iodide (Invitrogen) was used as a nuclear stain. Images were captured with a confocal laser scanning microscope (LSM510; Zeiss, Oberkochem, Germany). The experiments in Figs. 3, 4b, and 6a were performed independently at least three times, and representative results are shown.

Fertility test

Male and female mice aged 3 to 6 months old were placed in cages in pairs for mating. The females were checked daily for the presence of vaginal plugs and/or pregnancy. The females with the plugs were removed to holding cages to give birth. The size of each litter was recorded immediately after parturition.

Sperm number analysis

Male mice aged 12-17 weeks old were used. The cauda epididymis was removed, and four incisions were made in it to allow the spermatozoa to swim out. The cauda epididymis was then quickly transferred into a 15-ml centrifuge tube containing 2 ml of Toyoda Yokoyama Hoshi (TYH) medium (Mitsubishi Kagaku Iatron, Japan). After 30 min of incubation at 37˚C, the epididymal fragment was discarded, and the spermatozoa suspension was spun for 5 min (300 x *g* at RT). The precipitate was resuspended gently in 2 ml TYH medium. Spermatozoa were counted using a hemocytometer.

Sperm motility analyses

Mouse epididymal spermatozoa prepared as described above were used for a swim-up test. Five hundred microliters of spermatozoa at a concentration of 4 X 10^6/ml in TYH medium were aliquotted into ten 1.5-ml tubes. The samples were spun for 5 min (300 x *g* at RT), moved to a 37˚C incubator with 5% CO_2, and incubated for 0, 2, 5, 10, 15, 20, 30, 40, 50, or 60 min (one tube for each time point). An aliquot (20 µl) of the supernatant as close to the surface as possible in each tube was taken at each time point and the spermatozoa number was determined using a hemocytometer. Sperm movement was also quantified using the Sperm Motility Analysis System (SMAS, Kashimura Tokyo, Japan), a computer-assisted semen analysis (CASA) system, as described by Komori et al. (2006).

Statistical analyses

Results are represented as the mean $\pm$ SD from the number of experiments indicated in the legend to Figs. 5 and 8. Statistical differences were analyzed using the two-tailed unpaired Student's *t*-test (Figs. 5c, 8a, and 8b), a chi-square test (Table 1), or a two-way ANOVA test (Fig. 8c). Values of $p < 0.05$ were considered to be statistically significant.

Results

Targeted disruption of the mouse *Jlp* gene

We constructed a targeting vector designed to replace the first exon of the mouse *Jlp* gene with the neo cassette (Fig. 1a). ES cells containing the targeted allele were used to generate chimeric mice, and germ-line transmission of the targeted allele was achieved. Southern blot analysis confirmed the successful targeting of the *Jlp* gene (Fig. 1b). There was no detectable JLP protein in the testis of the *Jlp*-deficient mice (Fig. 1c). The homozygous ($Jlp^{-/-}$) mice, obtained by crossing the heterozygotes, were born with the expected Mendelian frequency, were viable, and appeared normal. No obvious phenotypic differences were observed between the wild-type and $Jlp^{-/-}$ mice. In addition, the $Jlp^{-/-}$ mouse testes appeared normal, both morphologically and histologically.

Western blotting and immunohistochemical analyses of JLP expression in the testis and epididymis of mouse and macaque

We first examined the expression of JLP in various tissues of the adult mouse by Western blotting analysis. As shown in Fig. 2, endogenous JLP comigrating with transiently expressed Flag-tagged JLP was expressed nearly ubiquitously, with its highest expression level being in the testis. Moderate or low expression was seen in the brain, lung, spleen, and ovary, and very low expression was seen in the heart, liver, kidney epididymis, and uterus.

We further analyzed JLP expression in the testis by immunohistochemistry. The anti-JLP antibody was specific, because no immunolabeling was seen in the *Jlp*-deficient testis (Fig. 3a, lower panel). Immunopositive signals were detected within the seminiferous tubules, in spermatocytes and spermatids, on wild-type testis sections, and the most intense immunosignals were in the elongated spermatids (Fig. 3a, upper panel). In addition, no

significant immunolabeling was detected in the cauda epididymis or epididymal sperm by immunohistochemistry (Fig. 3b; data not shown).

Next we asked whether mouse SPAG9, the product of a splice variant of the *Jlp* mRNA, is expressed in the testis and/or epididymis, and if so, whether its expression profile was similar to that of primate SPAG9. To examine this issue, we prepared cell lysates from the testes of adult mouse and macaque as well as from whole (for mouse) or cauda (for macaque) epididymides, and performed a Western blotting analysis. We used Flag-tagged mouse JLP and SPAG9 proteins transiently expressed in HEK293T cells as controls (Fig. 4a). The control Flag-JLP and -SPAG9 proteins were distinct and had different mobilities on SDS-PAGE (Fig. 4a, lanes 1 and 2). No proteins that co-migrated with Flag-SPAG9 were detected in the testes or epididymides of mouse and macaque, and the strongest bands in the testis samples migrated with a mobility indistinguishable from that of Flag-JLP in both mouse and macaque (Fig. 4a, lanes 3-6). However, because the open reading frame of macaque SPAG9 encodes 74 amino acids fewer than that of mouse SPAG9 (Jagadish et al., 2005b; GenBank accession numbers AF327451 and AB367798), a weak band in the macaque testis sample that migrated slightly faster than the control Flag-SPAG9 may represent macaque SPAG9 (Fig. 4a, lane 5). We also examined the adult macaque testis and cauda epididymis by immunohistochemistry (Fig. 4b). The spermatocytes and spermatids were strongly immunolabeled in the testis, and no immunosignals were detected in the cauda epididymis under our experimental conditions.

Expression of *Jlp* and *Spag9* mRNAs in mouse testis

We analyzed the expression of *Jlp* and *Spag9* mRNAs in mouse testis by RT-PCR. For this experiment, we employed two primer sets, Primers 1 and 2, and Primers 1 and 3, which specifically amplify the *Jlp* and *Spag9* cDNAs, respectively (see Figure 5a). As shown in Figure 5b, the reverse-transcription polymerase chain reaction (RT-PCR) using primer sets

specific for either the *Jlp* or *Spag9* cDNA (see Figure 5a), gave rise to the expected 150-bp bands, and the expression level of *Jlp* was higher than that of *Spag9*. To quantify the expression of these mRNAs, we further analyzed the *Jlp* and *Spag9* mRNAs by real-time RT-PCR. The result showed that the expression level of *Jlp* mRNA was approximately 10 times higher than that of Spag9 mRNA (Figure 5c).

Immunohistochemical and Western blotting analyses of JLP expression in the mouse testis during development

To examine the expression of JLP protein in the testis during development, we analyzed testis sections from mice on postnatal day (P) 10 (P10), P20, P30, and P40 by immunohistochemistry (Fig. 6a). JLP immunosignals were detected in all the samples examined, and the immunopositive cells were spermatogonia, spermatocytes, and spermatids. In particular, intense immunolabeling was observed in the elongated spermatids. We also performed Western blotting analysis of testis samples from mice at the same ages, in addition to the adult (12-weeks old). JLP expression was detected by Western blotting in the P10 mouse, and its expression level increased gradually with development, reaching a maximum at P40 (Fig. 6b, lanes 1-4). The expression level of JLP in the P40 and 12-week-old mouse samples was similar (Fig. 6b, lanes 4 and 5), indicating that JLP expression in the testis is maintained into adulthood.

Effect of *Jlp*-deficiency on the JNK signaling pathway

We asked whether ablation of the scaffold protein JLP would affect JNK signaling. To examine this issue, we analyzed the expression levels of P-JNK in tissues and cells of wild-type and *Jlp*-deficient mice by Western blotting, using an anti-phospho-JNK antibody. As shown in Figure 7a, the expression level of P-JNK was below detection in the $Jlp^{-/-}$

mouse testis (lanes 6 and 7). By contrast, its expression was substantial in the brain samples of both the wild-type and *Jlp*-deficient mice, and the levels of P-JNK were similar (lanes 8 and 9).

To determine if the loss of JLP perturbed the normal JNK activation response to stimuli, we used MEFs from wild-type and $Jlp^{-/-}$ mice. After exposing the MEFs to UV irradiation, osmotic stress, or anisomycin treatment, we analyzed the JNK signal by Western blotting. For all of these conditions, both the 54-kDa and 46-kDa isoforms of P-JNK were clearly detected, and there were no obvious differences between the levels in wild-type and $Jlp^{-/-}$ MEFs (Figure 7b).

Reduced fertility of *Jlp*-deficient male mice

To examine the physiological relevance of JLP expression in the testis, we investigated the fertility of the *Jlp*-deficient male mice (Table 1). Females were checked for the presence of vaginal plugs, and the success of the pregnancy was evaluated by the birth of offspring. Although $Jlp^{+/-}$ males were fully fertile (i.e., 96.2% of verified matings led to a successful pregnancy), the $Jlp^{-/-}$ males showed significantly reduced fertility (24.4%) when crossed with either $Jlp^{+/-}$ or $Jlp^{+/+}$ females. In contrast, $Jlp^{-/-}$ females crossed with $Jlp^{+/-}$ or $Jlp^{+/+}$ males did not show a significant loss of fertility. Taken together, these results suggest that the subfertility of the $Jlp^{-/-}$ male mice was probably due to poor quality and/or a reduced quantity of spermatozoa.

Characterization of spermatozoa in the *Jlp*-deficient mice

To examine the reason for the subfertility of the *Jlp*-deficient males, we compared the quantity of spermatozoa retrieved from their cauda epididymis with that of wild-type mice. As shown in Fig. 8a, the *Jlp* mutant mice produced approximately 60% as many

spermatozoa as wild-type mice. Next, we assessed the motility of the cauda epididymal spermatozoa by SMAS, a CASA system, and the swim-up test (Figs. 8b and 8c). No significant difference in the velocities of the $Jlp^{+/+}$ and $Jlp^{-/-}$ male spermatozoa was observed by SMAS analysis (Fig. 8b), in which spermatozoa were placed in a horizontal chamber. However, when we measured their vertical movement against gravity by the swim-up test, JLP-negative spermatozoa showed reduced motility compared with wild-type spermatozoa (Fig. 8c).

Discussion

In the present study, we examined the expression of the scaffold protein JLP in the testes of mice at different ages by immunohistochemical and Western blotting analyses. We also generated *Jlp*-deficient mice, and found that the male homozygotes were subfertile. To our knowledge, this study is the first to analyze the expression of JLP in the mouse testis during development and to suggest its importance in the production of functional spermatozoa in mice.

A specific probe is crucial for the accurate analysis of expression. To evaluate the specificity of the anti-JLP antibody used in this study, we used samples from the *Jlp*-deficient mice as controls for the Western blotting and immunohistochemical analyses. No proteins were labeled with this antibody in tissue sections from these mice, and no band with the same mobility as JLP was labeled on Western blots, confirming that our probe was specific, and that the data accurately reflected the JLP expression patterns in wild-type animals. In addition, consistent with a previous observation (Lee et al., 2002), we found that JLP was expressed in all the tissues we tested in wild-type mice, with its highest expression level being in the testis.

Specific immunohistochemical signals were also obtained in the testis. Although all the germ cells, i.e. spermatogonia, spermatocytes, and spermatids, were immunopositive, the most intense signals were in the elongated spermatids. This expression profile is distinct from that of JLP family member JSAP1, whose expression in the testis is exclusively in spermatogonia and spermatocytes, but not in spermatids (Bayarsaikhan et al., 2006). JLP and JSAP1, therefore, may play collaborative roles as scaffolding proteins in the early stages of spermatogenesis; in late stages, however, and especially in the elongated spermatids, JLP's role is likely to be independent of JSAP's.

In primates, SPAG9 is reported to be expressed exclusively in the testis, and to be localized specifically to the surface of spermatozoa (Shankar et al., 1998; Shankar et al.,

2004; Jagadish et al., 2005a and 2005b). Because the anti-JLP antibody used in our study was raised against a region in JLP that is mostly (~80%) common to both JLP and SPAG9 (see Materials and methods), it recognizes both proteins. Because of this, we distinguished between exogenously expressed Flag-tagged SPAG9 and JLP on Western blots probed with this antibody by the sizes of the bands. The expression level of the endogenous SPAG9 protein in the mouse testis, however, was below the level of detection, and the strongest band detected with the antibody was JLP. In addition, little or no expression of any protein was detected in the mouse cauda epididymis or epididymal spermatozoa by immunohistochemistry. These results may suggest that the mechanism(s) regulating the alternative splicing of the *Jlp* gene products are totally different between mouse and primates. However, this possibility is unlikely for the following reason: The macaque testis and cauda epididymis showed essentially the same expression profile as those of mice, using our antibody. That is, we found the highest immunoreactivity was with the JLP band, but not with SPAG9 in the macaque testes by Western blotting, and there were no significant immunosignals in the cauda epididymides by immunohistochemistry. However, we cannot rule out the possibility that our antibody to JLP does not recognize macaque JLP and SPAG9 proteins equally well. Because of this, further studies will be required to clarify the expression of primate JLP and SPAG9 in the testis and spermatozoa.

It is currently unclear why we were unable to detect SPAG9 protein, even in macaque testis, as the major JLP isoform. However, it is worth noting that the antibody used in this study on JLP recognizes both proteins, and previous studies on SPAG9 have used antibodies raised against the full-length SPAG9 protein (Shankar et al., 2004; Jagadish et al., 2005a and 2005b), which is also very likely to recognize JLP, given that almost the entire sequence of SPAG9, e.g. 758 amino acids out of 766 in humans (Shankar et al., 1998; Lee et al., 2002; GenBank accession number AF327452), is shared with JLP. This overlap in sequence complicates the study of the expression patterns and functional roles of these proteins, and may contribute to some of the apparent discrepancies between studies.

We observed no obvious phenotypic differences between the wild-type and *Jlp*$^{-/-}$ mice. In addition, the *Jlp*$^{-/-}$ mouse testes appeared morphologically and histologically normal. Thus, the functions of the scaffold protein JLP in vivo, with the exception of its affect on male fertility, may be largely compensated for by other scaffold proteins, such as JSAP1 and JNK-interacting protein 1 (JIP1). However, we cannot rule out the possibility that detailed analyses of the *Jlp*$^{-/-}$ mice might reveal physiological phenotypes. Furthermore, our study suggests that the scaffold JLP and its signal may be involved in the production of functionally normal spermatozoa, rather than in the structural construction of the testes. Further studies will be necessary to clarify these issues.

Our biochemical analyses showed that P-JNK was expressed at very low levels in the *Jlp*$^{-/-}$ mouse testis, but at a substantial level in the brain, and that the expression level of P-JNK in the brain was similar between wild-type and *Jlp*$^{-/-}$ mice. JLP-JNK signaling, therefore, may function generally in a cell-type-specific manner, or at specific stages of development or differentiation, and/or other scaffold proteins, such as JSAP1 and JIP1, may compensate for the loss of JLP scaffolding activity by activating JNK.

Here, we also evaluated the fertility of mice with a disrupted *Jlp* gene and found the JLP mutant homozygous males were subfertile. Although the SPAG9 message may also have been ablated in the transgenic animals, we feel comfortable attributing the subfertility phenotype to the loss of JLP because, in wild-type mice, the expression level of the *Spag9* mRNA was approximately one tenth of that of the *Jlp* mRNA by real-time RT-PCR, and no band of the appropriate size for SPAG9 was detectable by Western blotting. Finally, JLP and SPAG9 may have different transcription start sites, and it is therefore possible that the SPAG9 message was still transcribed in the *Jlp*-deficient transgenic mice.

In conclusion, our results indicate that the scaffold protein JLP, but not its splice variant SPAG9, is expressed intensely in the elongated spermatids in the mouse testis during development, and furthermore, that the ablation of JLP causes reduced fertility in male mice. Elucidation of the mechanisms underlying the reduced fertility may contribute greatly to our

understanding of how intracellular signaling pathways are involved in regulating spermatogenesis, a complex process, to produce the mature male gamete.

Acknowledgements

We thank Drs. H. Tanahashi, T. Yoshihara, and M Namiki (Kanazawa University) for helpful discussion and Y. Kawauchi (Toyama University) for technical assistance. This work was supported, in part, by grants-in-aid for scientific research from the Ministry of Culture, Sports, Science, and Technology of Japan.

References

Asano M, Furukawa K, Kido M, Matsumoto S, Umesaki Y, Kochibe N, Iwakura Y (1997) Growth retardation and early death of beta-1,4-galactosyltransferase knockout mice with augmented proliferation and abnormal differentiation of epithelial cells. EMBO J 16:1850-1857

Bayarsaikhan M, Shiratsuchi A, Gantulga D, Nakanishi Y, Yoshioka K (2006) Selective expression of the scaffold protein JSAP1 in spermatogonia and spermatocytes. Reproduction 131:711-719

Dhanasekaran DN, Kashef K, Lee CM, Xu H, Reddy EP (2007) Scaffold proteins of MAP-kinase modules. Oncogene 26:3185-3202

Friedrich G, Soriano P (1991) Promoter traps in embryonic stem cells: a genetic screen to identify and mutate developmental genes in mice. Genes Dev 5:1513-1523

Ito M, Yoshioka K, Akechi M, Yamashita S, Takamatsu N, Sugiyama K, Hibi M, Nakabeppu Y, Shiba T, Yamamoto K (1999) JSAP1, a novel Jun N-terminal protein kinase (JNK) that functions as scaffold factor in the JNK signaling pathway. Mol Cell Biol 19:7539-7548

Ito M, Akechi M, Hirose R, Ichimura M, Takamatsu N, Xu P, Nakabeppu Y, Shiba T, Yamamoto K, Yoshioka K (2000) Isoforms of JSAP1 scaffold protein generated through alternative splicing. Gene 255:229-234

Iwanaga A, Sato T, Sugihara K, Hirao A, Takakura N, Okamoto H, Asano M, Yoshioka, K (2007) Neural-specific ablation of the scaffold protein JSAP1 in mice causes neonatal death. Neurosci Lett 429:43-48

Jagadish N, Rana R, Selvi R, Mishra D, Garg M, Yadav S, Herr JC, Okumura K, Hasegawa A, Koyama K, Suri A (2005a) Characterization of a novel human sperm-associated antigen 9 (SPAG9) having structural homology with c-Jun N-terminal kinase-interacting protein. Biochem J 389:73-82

Jagadish N, Rana R, Selvi R, Mishra D, Shankar S, Mohapatra B, Suri A (2005b) Molecular cloning and characterization of the macaque sperm associated antigen 9 (SPAG9): an orthologue of human SPAG9 gene. Mol Reprod Dev 71:58-66

Kashef K, Lee CM, Ha JH, Reddy EP, Dhanasekaran DN (2005) JNK-interacting leucine zipper protein is a novel scaffolding protein in the Galpha13 signaling pathway. Biochemistry 44:14090-14096

Kelkar N, Gupta S, Dickens M, Davis RJ (2000) Interaction of a mitogen-activated protein kinase signaling module with the neuronal protein. JIP3. Mol Cell Biol 20:1030-1043

Kelkar N, Standen CL, Davis RJ (2005) Role of the JIP4 scaffold protein in the regulation of mitogen-activated protein kinase signaling pathways. Mol Cell Biol 25:2733-2743

Komori K, Tsujimura A, Ishijima S, Tanjapatkui P, Fujita K, Matsuoka Y, Takao T, Miyagawa Y, Takada S, Okuyama A (2006) Comparative study of sperm motility analysis system and conventional microscopic semen analysis. Reprod Med Biol 5:195-200

Lee CM, Onésime D, Reddy CD, Dhanasekaran N, Reddy EP (2002) JLP: A scaffolding protein that tethers JNK/p38MAPK signaling modules and transcription factors. Proc Natl Acad Sci USA 99:14189-14194

Morrison, DK, Davis RJ (2003) Regulation of MAP kinase signaling modules by scaffold proteins in mammals. Ann Rev Cell Dev Biol 19:91-118

Nguyen Q, Lee CM, Le A, Reddy EP (2005) JLP associates with kinesin light chain 1 through a novel leucine zipper-like domain. J Biol Chem 280:30185-30191

Sato S, Ito M, Ito T, Yoshioka K (2004) Scaffold protein JSAP1 is transported to growth cones of neurites independent of JNK signaling pathways in PC12h cells. Gene 329:51-60

Sato T, Hidaka, K, Iwanaga A, Ito M, Asano M, Nakabeppu Y, Morisaki T, Yoshioka K (2005) Impairment of cardiomyogenesis in embryonic stem cells lacking scaffold protein JSAP1. Biochem Biophys Res Commun 338:1152-1157

Shankar S, Mohapatra B, Suri A (1998) Cloning of a novel human testis mRNA specifically expressed in testicular haploid germ cells, having unique palindromic sequences and encoding a leucine zipper dimerization motif. Biochem Biophys Res Commun 243:561-565

Shankar S, Mohapatra B, Verma S, Selvi R, Jagadish N, Suri A (2004) Isolation and characterization of a haploid germ cell specific sperm associated antigen 9 (SPAG9) from the baboon. Mol Reprod Dev 69:186-193

Takaesu G, Kang JS, Bae GU, Yi MJ, Lee CM, Reddy EP, Krauss RS (2006) Activation of p38α/β MAPK in myogenesis via binding of the scaffold protein JLP to the cell surface protein Cdo. J Cell Biol 175:383-388

Yagi T, Nada S, Watanabe N, Tamemoto H, Kohmura N, Ikawa Y, Aizawa S (1993) A novel negative selection for homologous recombinants using diphtheria toxin A fragment gene. Anal Biochem 214:77-86

Yoshioka K (2004) Scaffold proteins in mammalian MAP kinase cascades. J Biochem 135:657-661

Figure legends

Fig. 1 Targeted disruption of the mouse *Jlp* gene. (**a**) Schematic illustration of the targeting of the mouse *Jlp* gene. B, *Bam*HI; E, *Eco*RI; M, *Mlu*I; N, *Not*I; Nh, *Nhe*I; S, *Sal*I; neo, neomycin-resistant cassette; DT-A, *diphtheria* toxin-A gene. (**b**) Southern blot analysis of $Jlp^{+/+}$, $Jlp^{+/-}$, and $Jlp^{-/-}$ mice. Genomic DNA isolated from the mice (12 weeks old) was digested with *Nhe*I and *Mlu*I (for the P1 probe) or with *Bam*HI (for the neo probe), and subjected to Southern blotting with the 5'-flanking P1 fragment (left panel) and the neo fragment (right panel) indicated in (**a**) as probes. (**c**) Cell lysates (20 µg/lane) from the testes of 12-week-old $Jlp^{+/+}$ and $Jlp^{-/-}$ mice were analyzed by Western blotting with an anti-JLP antibody (upper lane). The positions of the protein size markers are indicated on the left. The actin band served as a loading control (lower panel).

Fig. 2 Expression of JLP in mouse tissues. Cell lysates (20 µg/lane) prepared from various tissues of a 12-week-old mouse were analyzed by Western blotting with the anti-JLP antibody (upper lane). Flag-tagged JLP was transiently expressed in HEK293T cells and the cell lysate was used as a control (upper panel, lane 1). The positions of the protein size markers are indicated on the left. The actin band served as a loading control (lower panel).

Fig. 3 Immunohistochemistry of sections from the testis (10-µm thick) (**a**) and cauda epididymis (20-µm thick) (**b**) of 12-week-old $Jlp^{+/+}$ and $Jlp^{-/-}$ mice, stained with an anti-JLP antibody (*green*) and TOTO-3 (*blue*). TOTO-3 was used as a nuclear stain. Immunopositive signals within the seminiferous tubules on the wild-type testis section were detected in spermatocytes and spermatids, and the most intense immunosignals were in the elongated spermatids. No significant immunolabeling was observed in the cauda epididymis. Scale bars, 50 µm. Inset panels in (**b**) show overexposed, lower-magnification photos of the same areas.

Fig. 4 (**a**) Western blotting analysis of the testes and epididymides of mouse and macaque. Cell lysates (20 μg/lane) prepared from the testis of mouse (12 weeks old) and macaque (96 months old) as well as whole (for mouse) or cauda (for macaque) epididymides were analyzed by Western blotting with the anti-JLP antibody (upper panel). Flag-tagged mouse JLP and SPAG9 proteins were transiently expressed in HEK293T cells, and the cell lysates were used as controls (upper panel, lanes 1 and 2). The positions of the protein size markers are indicated on the left. The actin band served as a loading control (lower panel). (**b**) Immunohistochemistry of the testis (10-μm) and cauda epididymis (20-μm) sections from a macaque (70 months old) stained with the anti-JLP antibody (*green*) and TOTO-3 (*blue*). Intense signals were observed in the spermatocytes and spermatids. By contrast, no significant immunolabeling was detected in the cauda epididymis. The upper right panel, TOTO-3 (enlarged), is the high-magnification view of the area indicated in the upper second panel from the left, TOTO-3. The white open arrowhead and closed arrowhead indicate a spermatid and spermatocyte, respectively. Scale bars, 50 μm.

Fig. 5 Expression of *Jlp* and *Spag9* mRNAs in mouse testis. (**a**) Schematic illustration of the *Jlp* and *Spag9* mRNAs generated from the mouse *Jlp/Spag9* gene. The primer sets, Primers 1/2 and Primers 1/3, were used to amplify *Jlp* and *Spag9* cDNAs, respectively. (**b**) Total RNAs were prepared from adult mouse testes, and RT-PCR was carried out using specific primers for *Jlp* (lanes 1 and 3) or *Spag9* (lanes 2 and 4) cDNAs. As a control, the reactions shown in lanes 1 and 2 did not include the reverse-transcription step. The arrow indicates the position of the PCR products (both 150-bp in size) derived from the cDNAs of *Jlp* and *Spag9*. M, DNA size markers. (**c**) Real time RT-PCR analysis of *Jlp* and *Spag9* mRNAs. *Jlp* and *Spag9* expression levels were normalized to that of *Gapdh* mRNA (means + SD from 3 experiments, $*p < 0.01$, Student's *t*-test).

Fig. 6 Immunohistochemical (**a**) and Western blotting (**b**) analyses of JLP expression in the testis during development. (**a**) Sections (10-μm thick) cut from the testes of mice at P10, P20, P30, and P40, were stained with an anti-JLP antibody (*green*) and TOTO-3 (*blue*). Scale bar, 50 μm. (**b**) Cell lysates (6 μg/lane) from the testes of mice at the same ages and a 12-week-old (12wk) mouse, were subjected to Western blotting analysis and probed with the anti-JLP antibody (upper lane). The positions of protein size markers are indicated on the left. The actin band served as a loading control (lower panel).

Fig. 7 (**a**) Expression of active JNK in the testis and brain of wild-type and *Jlp*-deficient mice. Cell lysates (20 μg/lane) prepared from the testis and brain of $Jlp^{+/+}$ and $Jlp^{-/-}$ mice (12 weeks old) were analyzed by Western blotting with the anti-JLP antibody (upper panel, lanes 2-5), or anti-phospho-JNK antibody (upper panel, lanes 6-7). Flag-tagged mouse JLP protein was transiently expressed in HEK293T cells, and the cell lysate was used as a control (lane 1). **(b)** Activation of JNK in MEFs derived from $Jlp^{+/+}$ and $Jlp^{-/-}$ mice. MEFs were not stimulated (ctrl), or were stimulated by UV-C irradiation (UV), sorbitol (Sorb), or anisomycin (Aniso). Cell lysates (20 μg/lane) prepared from the MEFs were analyzed by Western blotting with the anti-JLP antibody (upper panel, lanes 1 and 2), or anti-phospho-JNK antibody (upper panel, lanes 3-10). The actin band served as a loading control (lower panels). P-JNK54, P-JNK p54 kDa isoform; P-JNK46, P-JNK p46 kDa isoform.

Fig. 8 Characterization of epididymal spermatozoa in the *Jlp*-deficient mice. (**a**) Counts of cauda epididymal spermatozoa recovered from the $Jlp^{+/+}$ and $Jlp^{-/-}$ male mice (means $\pm$ SD from 7 experiments, $*p < 0.01$, Student's *t*-test). (**b, c**) Analyses of spermatozoa prepared from the cauda epididymides of $Jlp^{+/+}$ and $Jlp^{-/-}$ male mice by the SMAS (b) and swim-up test (c). No significant difference in the velocity of $Jlp^{+/+}$ and $Jlp^{-/-}$ male spermatozoa was observed by SMAS analysis (means $\pm$ SD from 3 experiments). In the swim-up test,

however, the JLP-negative spermatozoa showed significantly less motility than wild-type spermatozoa. (c) The number of spermatozoa in an aliquot (20 μl) that swam to the top of the supernatant after centrifugation by the time point indicated (means ± SD from 3 experiments, #$p < 0.01$, two-way ANOVA).

Supplementary Fig. 1. Comparison of sizes of Flag-tagged mouse JLP, mouse SPAG9, and macaque SPAG9 proteins. Expression plasmids for Flag-tagged mouse JLP, mouse SPAG9, and macaque SPAG9 protein, Flag-JLP(mouse), Flag-SPAG9(mouse), and Flag-SPAG9(macaque), respectively, were transiently expressed in HEK293T cells, and the cell lysates were analyzed by Western blotting with an anti-Flag antibody. The positions of the protein size markers are indicated at left.

Table 1

Fertility of *jlp*-deficient mice

jlp genotype		No.	No.	Mean litter
Male	Female	crossings	pregnancies (%)	sizes (± SD)
+/-	+/+, +/-	26	25 (96.2)	8.5 (± 2.1)
-/-	+/+, +/-	41	10 (24.4)*	6.4 (± 1.6)
+/+, +/-	-/-	12	10 (83.3)	6.9 (± 1.4)

Mean litter size was calculated as the number of live pups born per number of litters.

*$p < 0.01$, chi-square test.

Figure 1

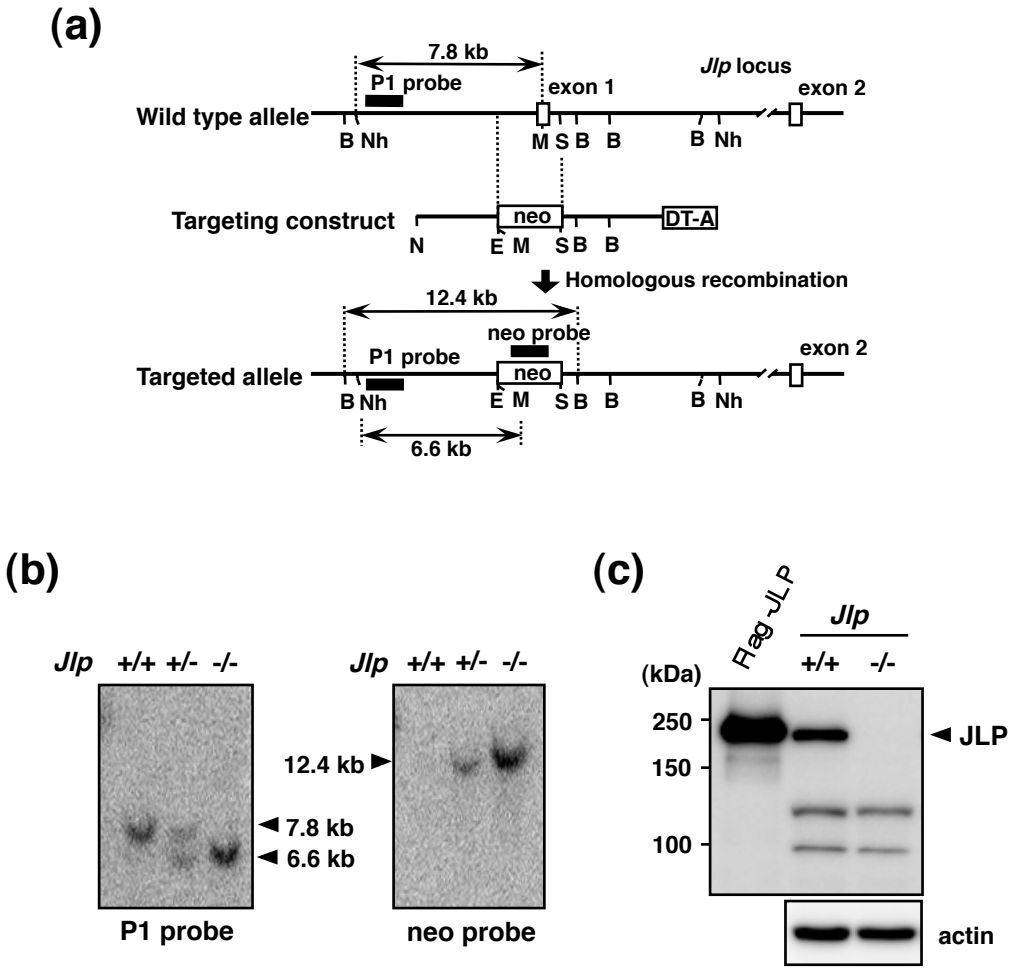
(a)
7.8 kb
P1 probe
Jlp locus
exon 1
exon 2
Wild type allele
B Nh
M S B B
B Nh
Targeting construct
neo
DT-A
N
E M S B B
Homologous recombination
12.4 kb
neo probe
P1 probe
exon 2
Targeted allele
neo
B Nh
E M S B B
B Nh
6.6 kb
(b)
Jlp +/+ +/- -/-
Jlp +/+ +/- -/-
12.4 kb
7.8 kb
6.6 kb
P1 probe
neo probe
(c)
Reg-JLP
Jlp
+/+ -/-
(kDa)
250
150
100
JLP
actin

Figure 2

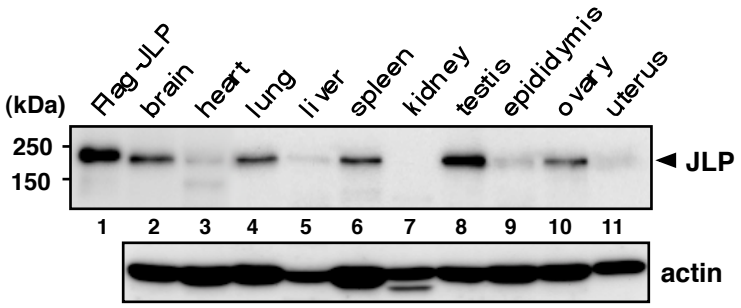
Flag-JLP
brain
heart
lung
liver
spleen
kidney
testis
epididymis
ovary
uterus
(kDa)
250
150
JLP
1 2 3 4 5 6 7 8 9 10 11
actin

Figure 3

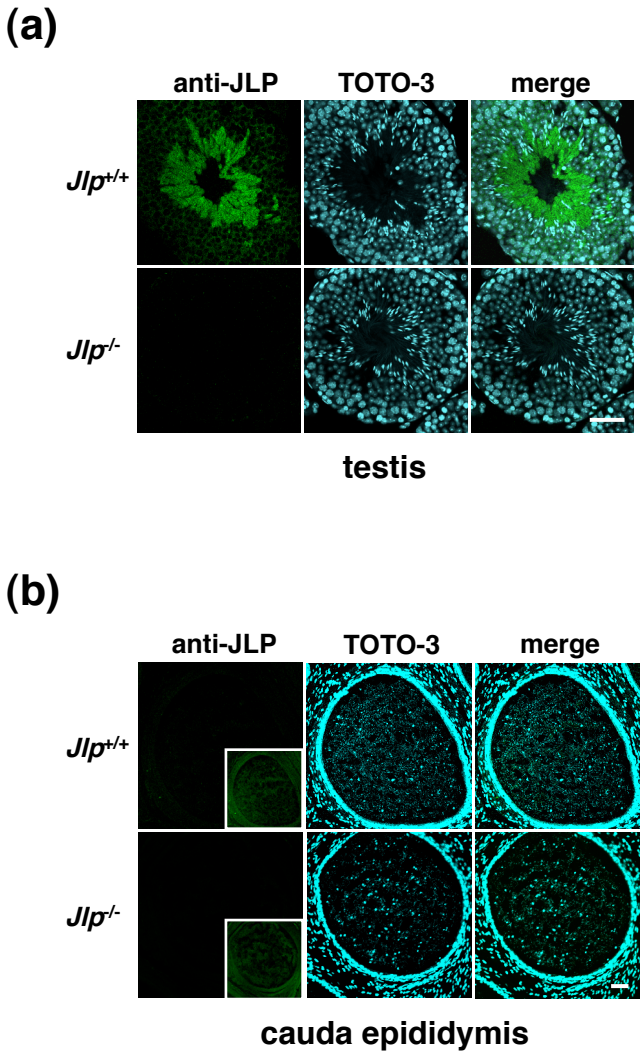
(a)
anti-JLP
TOTO-3
merge
Jlp+/+
Jlp-/-
testis
(b)
anti-JLP
TOTO-3
merge
Jlp+/+
Jlp-/-
cauda epididymis

Figure 4

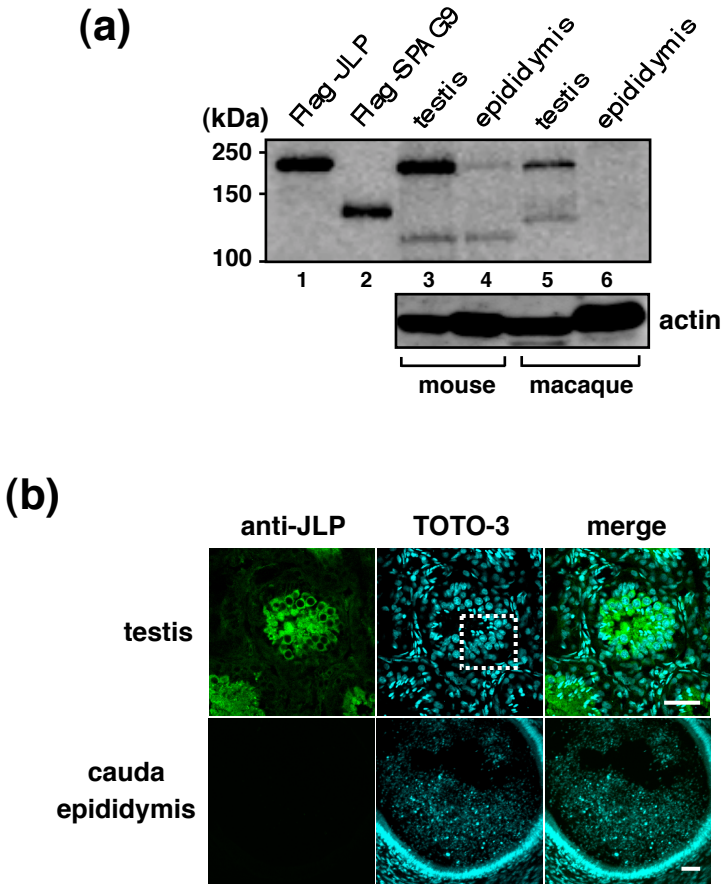
(a)
Flag-JLP
Flag-SPAG9
testis
epididymis
testis
epididymis
(kDa)
250
150
100
1
2
3
4
5
6
actin
mouse
macaque
(b)
anti-JLP
TOTO-3
merge
TOTO-3
(enlarged)
testis
cauda
epididymis

Figure 5

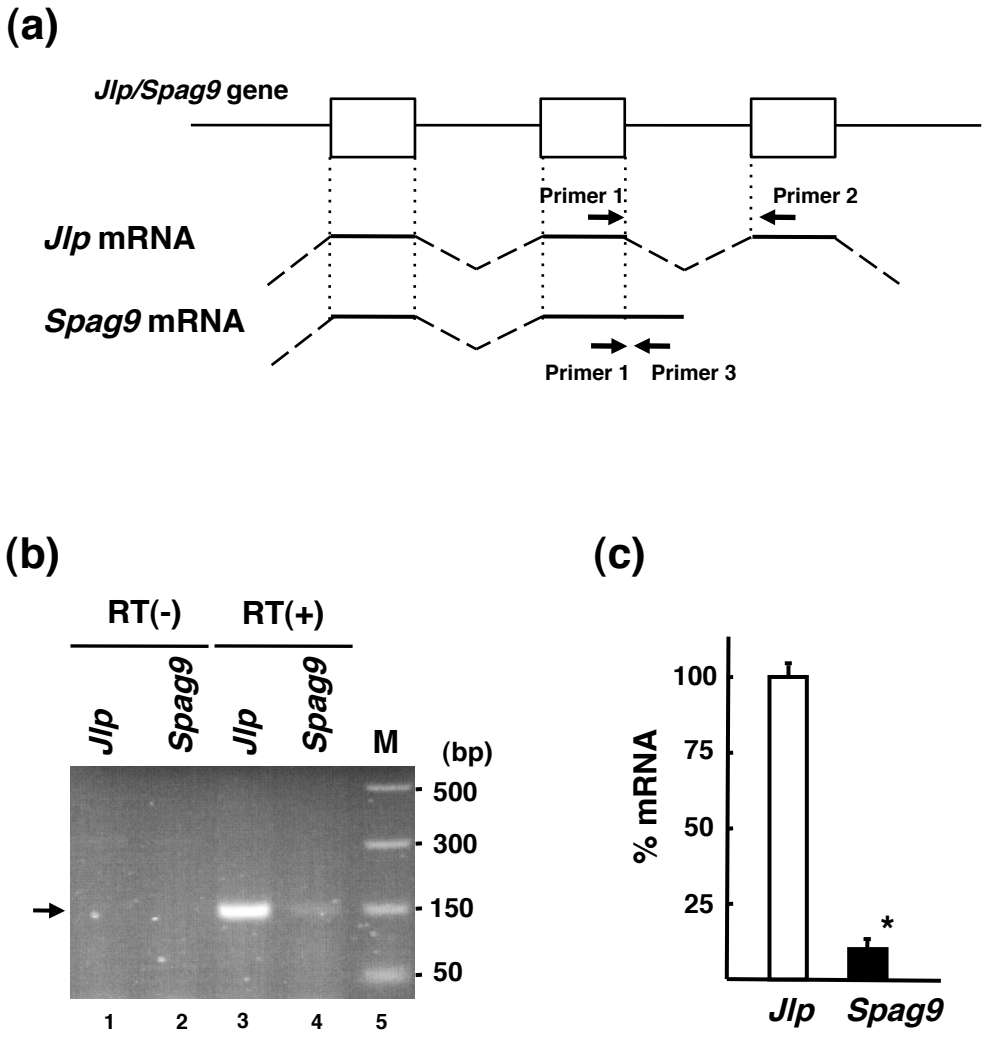
(a)
Jlp/Spag9 gene
Primer 1
Primer 2
Jlp mRNA
Spag9 mRNA
Primer 1
Primer 3
(b)
RT(-)
RT(+)
Jlp
Spag9
Jlp
Spag9
M
(bp)
500
300
150
50
1
2
3
4
5
(c)
100
75
50
25
% mRNA
*
Jlp
Spag9

Figure 6

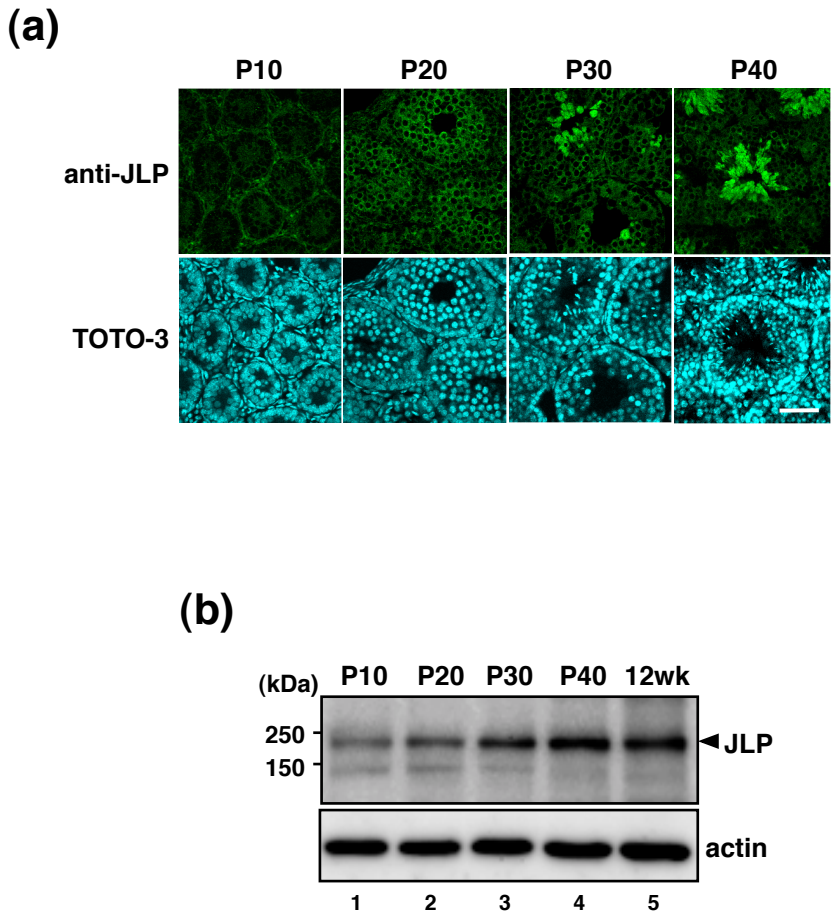
(a)
P10
P20
P30
P40
anti-JLP
TOTO-3
(b)
(kDa)
P10
P20
P30
P40
12wk
250
150
JLP
actin
1
2
3
4
5

Figure 7

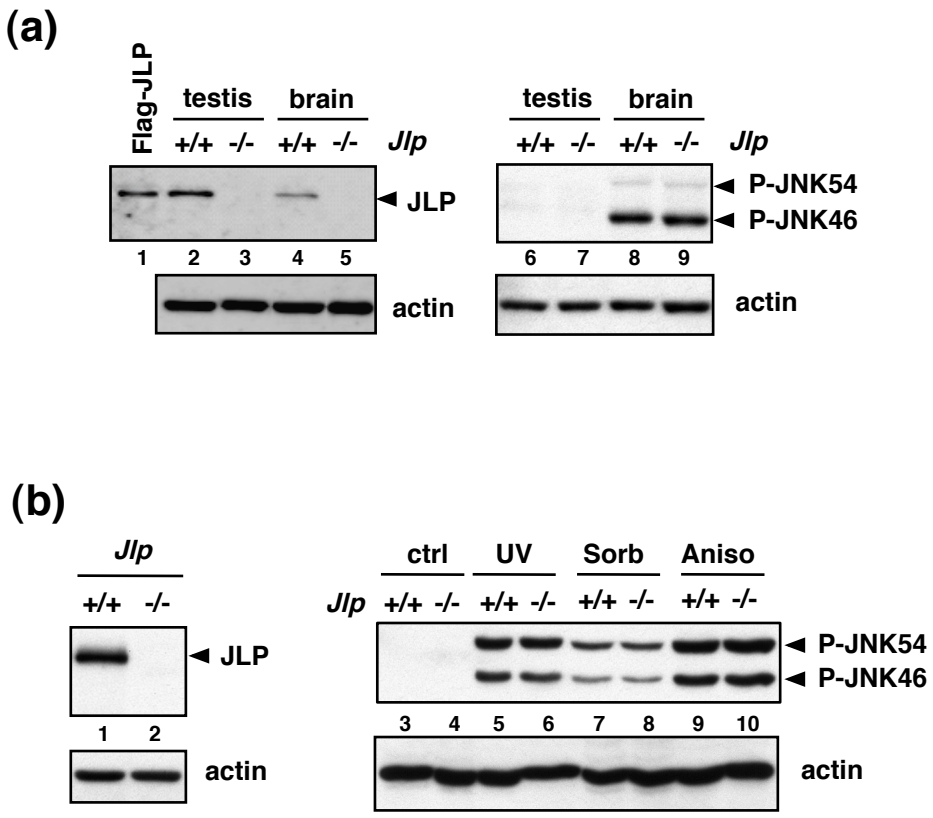
(a)
Flag-JLP
testis
brain
+/+ -/- +/+ -/-
Jlp
JLP
1 2 3 4 5
actin
testis
brain
+/+ -/- +/+ -/-
Jlp
P-JNK54
P-JNK46
6 7 8 9
actin
(b)
Jlp
+/+ -/-
JLP
1 2
actin
ctrl
UV
Sorb
Aniso
Jlp +/+ -/- +/+ -/- +/+ -/- +/+ -/-
P-JNK54
P-JNK46
3 4 5 6 7 8 9 10
actin

Figure 8

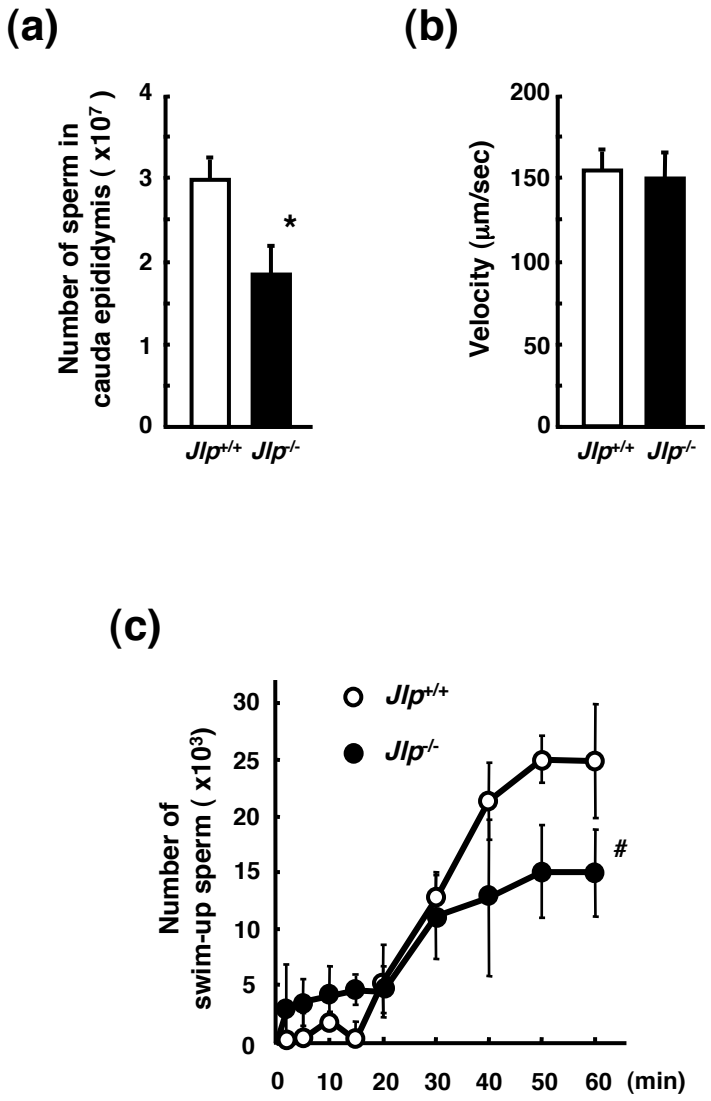
(a)
Number of sperm in cauda epididymis (x10^7)
4
3
2
1
0
*
Jlp+/+
Jlp-/-
(b)
Velocity (μm/sec)
200
150
100
50
0
Jlp+/+
Jlp-/-
(c)
Number of swim-up sperm (x10^3)
30
25
20
15
10
5
0
Jlp+/+
Jlp-/-
#
0
10
20
30
40
50
60
(min)

Supplementary Figure 1